Journal of Nuclear Materials 409 (2011) 18–26

Contents lists available at ScienceDirect

Journal of Nuclear Materials

journal homepage: www.elsevier.com/locate/jnucmat

Effect of ion irradiation-produced defects on the mobility of dislocations in 304 stainless steel

M. Briceño [a], J. Fenske [a], M. Dadfarnia [b], P. Sofronis [b], I.M. Robertson [a,*]

[a] Department of Materials Science and Engineering, University of Illinois, Urbana, IL 61801, United States
[b] Department of Mechanical Science and Engineering, University of Illinois, Urbana, IL 61801, United States

ARTICLE INFO

Article history:
Received 17 September 2010
Accepted 8 December 2010
Available online 17 December 2010

ABSTRACT

The impact of heavy-ion produced defects on the mobility of dislocations, dislocation sources and newly generated dislocations in 304 stainless steel are discovered by performing irradiation and deformation experiments in real time in the transmission electron microscope. Dislocations mobile prior to the irradiation are effectively locked in position by the irradiation, but the irradiation has no discernible impact on the ability of a source to generate dislocations. The motion and mobility of a dislocation is altered by the irradiation. It becomes irregular and jerky and the mobility increases slowly with time as the radiation-produced defects are annihilated locally. Channels created by dislocations ejected from grain boundary dislocation sources were found to have a natural width, as the emission sites within the boundary were spaced close together. Finally, the distribution of dislocations, basically, an inverse dislocation pile-up, within a cleared channel suggests a new mechanism for generating high local levels of stress at grain boundaries. The impact of these observations on the mechanical properties of irradiated materials is discussed briefly.

1. Introduction

The degradation of the mechanical properties of metals following exposure to irradiation with energetic particles, such as neutrons, protons and heavy-ions, is well documented [1–10]. The degradation appears as a loss of ductility; an increase in the yield strength, even to the point of establishing a distinct yield point drop in face-centered cubic metals; and an increase in the tensile strength. These responses are independent of the crystal structure (BCC, FCC and HCP), material purity (pure metals and alloys), and the nature of the energetic particle (electrons, ions, protons and neutrons) used to create the damage. Post-deformation examination of the microstructure shows the black dot damage (small interstitial and vacancy loops) typical of an irradiated material with channels that are partially and perhaps fully cleared of defects [11,12]. Within a channel, isolated dislocations as well as tangled configurations of dislocations exist. Unifying these observations with the macroscopic mechanical properties and developing a physically-based model that can predict even the degradation of the stress–strain behavior has been a challenge [4,7,8,13,14]. For example, Arsenlis et al., based on the key features garnered from experimental studies, developed a constitutive relationship that captured the salient features of degradation of the macroscopic stress–strain relationship [13]. However, even in this case key experimental effects had to be treated phenomenologically. The primary issue is a lack of understanding of the physical processes controlling the deformation and how these processes dictate the macroscopic properties.

Identifying the source of the dislocations responsible for making these channels, how these dislocations clean the channel of defects and how these dislocations interact with grain boundaries has important implications in understanding the physical processes governing irradiation-assisted stress corrosion cracking. Was and Busby have considered the various effects occurring under irradiation: production of a hardened matrix, formation of a defect-free channel, Cr depletion at grain boundaries, grain boundary structural modifications due to absorption of point defects, etc., and concluded that none of these effects by themselves can account for the susceptibility of stainless steels to stress corrosion cracking [15]. They concluded that an important component in determining why a grain boundary response transitioned from transmission of strain to grain boundary cracking was how the boundary accommodated the dislocations from the channels and responded to the local stress associated with the dislocation pile-up that formed.

Molecular dynamics computer simulations as well as dynamic deformation experiments *in situ* in the transmission electron microscope have shown the complex and numerous interactions that are possible between a mobile dislocation and an irradiation-produced defect [8,12,16–23]. Most recently these studies have focused on the interaction of dislocations with isolated stacking-fault tetrahedra, with the result that the interaction can

* Corresponding author.
E-mail address: ian.robertson@tcd.ie (I.M. Robertson).

0022-3115/$ - see front matter © 2010 Elsevier B.V. All rights reserved.
doi:10.1016/j.jnucmat.2010.12.026

annihilate a tetrahedron, shear it to produce smaller tetrahedra, interact with it to produce either a smaller tetrahedron or another type of defect. The details of the interaction are dependent on the character of the dislocation, edge or screw; the type of tetrahedron, truncated or full; and on the point of impact of the dislocation on the tetrahedron, face or on the stair-rod dislocations that border it. Few dynamic studies on the formation of the defect-free channels and the source of dislocations responsible for creating them have been conducted. Robach et al. provided limited direct evidence showing that pre-existing dislocations were immobile in ion irradiated material and that the dislocations responsible for forming the channels were generated from new sources, such as grain boundaries and stress concentrators such as crack tips [11]. Edwards et al. conducted post-deformation analysis and interpreted their observations using the same concepts [24]. However, several questions remain to be addressed, namely, the influence of the irradiation on the dislocation source, the mechanism by which the dislocations interacted with the obstacle field to create the cleared channels and how these dislocations interacted with and were accommodated in grain boundaries.

In this paper, the results of dynamic observations of the effects of heavy-ion irradiation on the room temperature behavior of mobile dislocations as well as dislocation sources in 304 stainless steel are reported. The observations were made in real time by conducting the heavy-ion irradiations as well as the deformation experiments *in situ* in a transmission electron microscope.

2. Experimental procedures

The starting material was 304 stainless steel foil with a thickness of approximately 150×10^{-6} m. Samples with dimensions of 11.5×10^{-3} m-long $\times$ 2.5×10^{-3} m-wide were cut from the foil, holes for attaching the sample to the straining stage drilled, and the samples annealed at 1060 °C for 30 min. The central section of these samples was thinned to electron transparency using a twin jet polisher and an electrolyte of 6% perchloric acid, 39% butanol and 55% methanol.

The ion irradiations as well as the deformation experiments were performed *in situ* in a transmission electron microscope using the IVEM-accelerator facility at Argonne National Laboratory. The samples were irradiated at room temperature with 1 MeV Kr ions to a dose in the range 0.5–5 $\times$ 10^{17} ions m^{-2}; this dose range was selected to give a reasonable defect density throughout the electron transparent foil. The *in situ* straining was accomplished using a single-tilt high-temperature straining stage (GATAN Model 672). The electron microscope, a Hitachi 9000 was operated at an accelerating voltage of 200 keV. The experimental approach involved straining prior to irradiation to create a population of mobile dislocations under this loading condition, irradiating and loading again or simply loading an irradiated sample.

3. Experimental results

The ion irradiation was with 1 MeV Kr^+ ions. With this energy the ions are not deposited in the thin foil and the energy lost is deposited primarily in the formation of sub-cascades, which will produce small defects throughout the foil thickness. The dark-field micrographs presented in Fig. 1 compare the microstructure in an unirradiated and irradiated (3×10^{17} ions cm^{-2}) foil. Clearly, the irradiation produces a high density of small defects that should be distributed throughout the foil. The type of defect was not determined in this study but based on the work of Cole and Bruemmer, the defects are expected to be small Frank loops [25].

The first experimental mode involved creating a set of mobile dislocations and then irradiating the sample to a dose of 3×10^{17} ions m^{-2} to determine if these dislocations remained mobile and if the dislocation source continued to generate dislocations with and without application of an additional applied stress. The bright-field micrographs shown in Fig. 2, compare the mobile dislocation structure generated prior but imaged immediately after the ion irradiation, Fig. 2a; the position after 335 s of a loading experiment, Fig. 2b; and after further significant loading, Fig. 2d. Here it is important to realize that the experimental method has no capability to measure the amount of displacement, and the only assessment that this region was under load was the observation of additional dislocation activity in this region; examples of this are shown in subsequent figures. To demonstrate the extent of dislocation motion, difference images, formed by superimposing a positive image of the initial position on a negative of a later state, were made and are presented as Fig. 2c and e for the two loading times. Both difference images show that any motion of these dislocations is negligible. That is, the damage created by the irradiation effectively locked the mobile dislocations in their pre-irradiation position.

The source that created the dislocations observed in Fig. 2 was near a crack tip located some distance behind them. With small

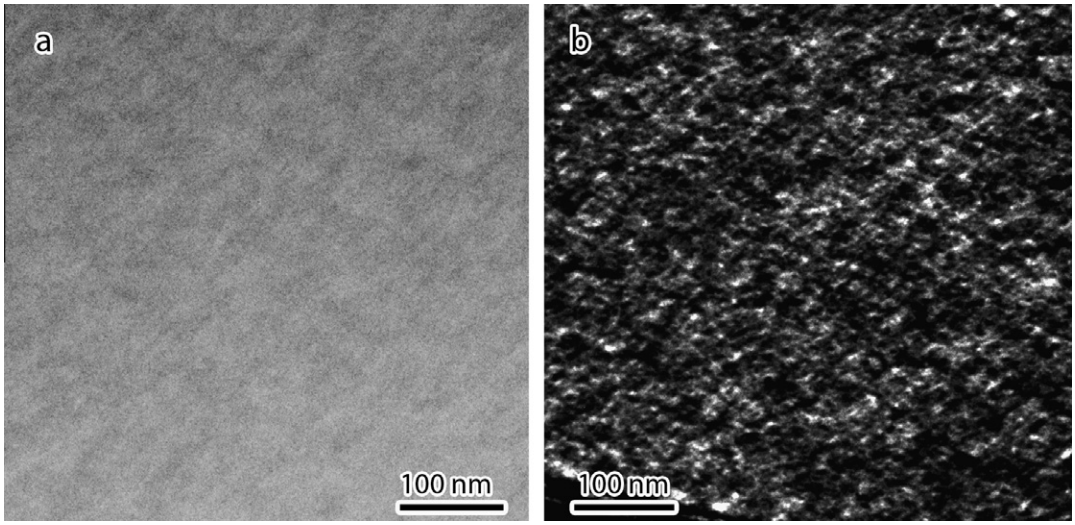

Fig. 1. Dark-field images of the unirradiated and irradiated microstructure. The damage was produced by a 1 MeV Kr^+ irradiation to a dose of 3×10^{17} m^{-2}.

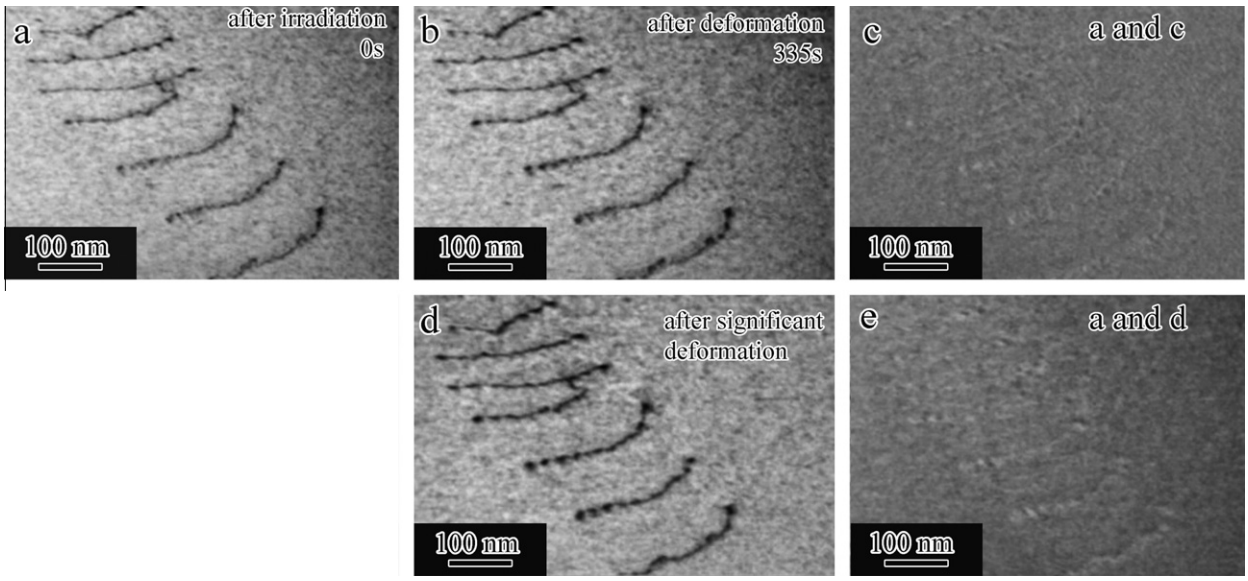

Fig. 2. Comparison of the position of the dislocations (a) immediately after irradiation, (b) after further straining, (c) difference image of a and b, (d) after significant straining, (e) difference image of a and d.

incremental increases in the applied stage displacement, this source continued to generate new dislocations on the original as well as on parallel slip systems. That is, the irradiation-produced defects appeared to have negligible impact on the ability of a source to nucleate new dislocations. However, there were several notable differences between these dislocations and the ones generated prior to the irradiation. The first was the distance the dislocations travelled from the source, which was notably less than in the unirradiated case. Evidence for this is that no new dislocations travelled to the position of the dislocations shown in Fig. 2 despite the generation of a significant number of dislocations on this slip plane. Another difference was in the dislocation activity and motion within the active slip band. It now occurred in a discontinuous manner, was slow and jerky as the dislocations percolated through and interacted with the irradiation-produced obstacles. These features are evident in the time-resolved images captured at different times in the deformation experiment and select examples are presented in Figs. 3–5. Difference images are again constructed to aid visualization of the motion and the distance moved. From these images it can be seen that:

- The motion of individual dislocations occurs in a segmented fashion, which is consistent with segments of the dislocation breaking free from the barriers at different times. This is

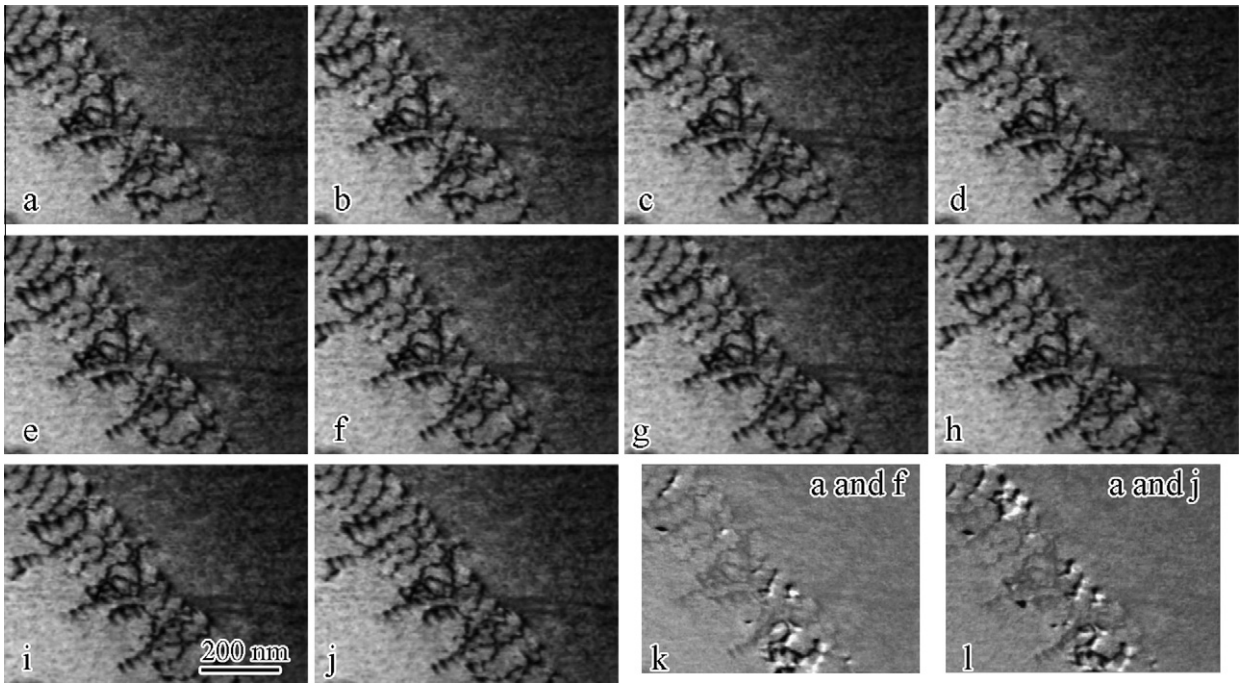

Fig. 3. Time-resolved series of images showing dislocation motion on the same slip band as in Fig. 1 immediately after irradiation. The time difference between each successive image was 10 s.

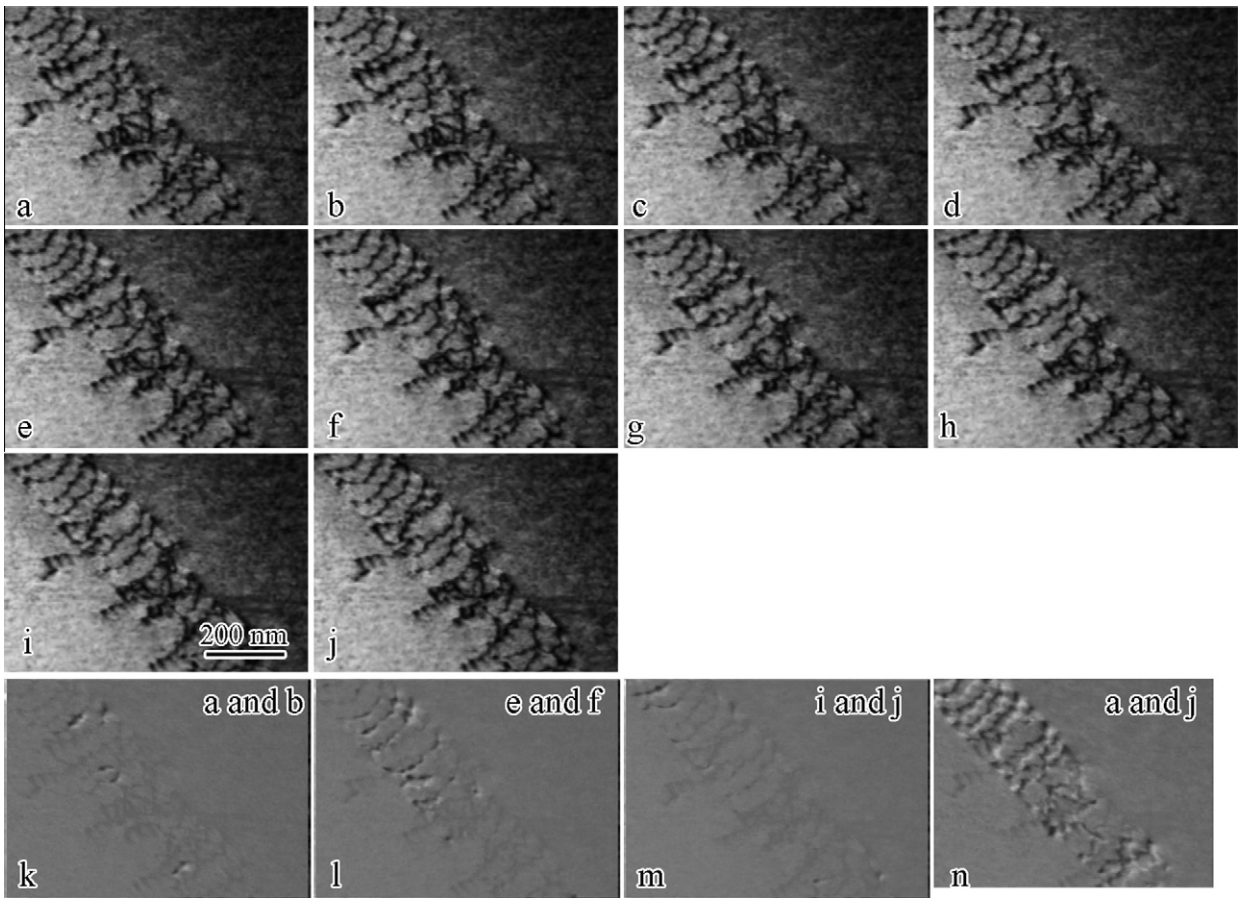

Fig. 4. Time-resolved series of images showing dislocation motion on the same slip band as in Fig. 1 after irradiation. The time difference between each successive image was 10 s.

expected as the barrier is not necessarily the same for the entire dislocation as it may intersect the barrier at different locations giving a range of barrier strengths. This segmented motion is particularly evident in the images presented in Fig. 3 in which only small segments of some dislocations are seen to move.

- The motion of one segment of a dislocation does not necessarily cause motion in neighboring dislocations as evidenced by the nature of the motion shown in Figs. 4k, 5l and n. This observation suggests that the dislocation interaction forces are insufficient to cause the dislocation to break free of the obstacle and/or that the dislocations never get sufficiently close to experience one another.
- Dislocation motion occurs in a discontinuous manner, as seen by the periods of inactivity that occur for some dislocations under constant load conditions; compare, for example, Figs. 4k, l and 5k–m.
- The degree of dislocation motion increases with time. This can be seen by comparing the dislocation motion in Figs. 3–5, which are at increasing times from a deformation pulse – that is the stage was pulsed and then held constant. In Fig. 3, in which the obstacle density is the greatest, the dislocations move in a segmented fashion with no evidence for motion of complete dislocations, Fig. 3l. In contrast in Figs. 4 and 5, which are for later periods and after significant dislocation motion, complete dislocations have moved. For some dislocations, motion of the entire dislocation line occurs within the 10 s timeframe between images; see the difference images in Figs. 4l and 5k and for others the motion is still in a segmented incremental manner. The projected distance moved in any time increment is not uniform and is between 5 and 20 nm. These effects are consistent with the mobile dislocations decreasing the obstacle strength through either annihilating the defect or reducing its size and thereby making an easy glide path. This would make it easier for subsequent dislocations to move through this area.
- This dislocation motion is different from that in unirradiated material as the outer segments are seen to move while the central segment remains locked in position. Normal motion in *in situ* TEM straining experiments in unirradiated foils has the central segment leading the outer segment because of the influence of surface image forces.

To illustrate the difference in the dislocation motion between the unirradiated and irradiated materials, a time-resolved series of images of dislocations approaching a grain boundary in the unirradiated material is shown in Fig. 6. The time between each image is 5 s so that the comparison of the initial and final positions, Fig. 6d, is equivalent to the time difference between successive images in Figs. 3–5. The difference image, Fig. 6d, shows mostly white dislocations indicating that they have entered the field-of-view during this time increment, which corresponds to them moving a distance of several hundred nanometers. Another obvious difference is in the shape of the dislocation line, it is now smooth and uniform compared to in the irradiated case. Furthermore, the line moves as a unit as opposed to the segmented motion seen in the irradiated material. The curvature of the dislocations seen in Fig. 6 is a direct consequence of the free surface pinning the outer segments of the dislocations.

The difference in the motion of dislocations in the slip band and the distribution suggests that the nature of dislocation pile-ups formed at grain boundaries may be different in the two cases. To

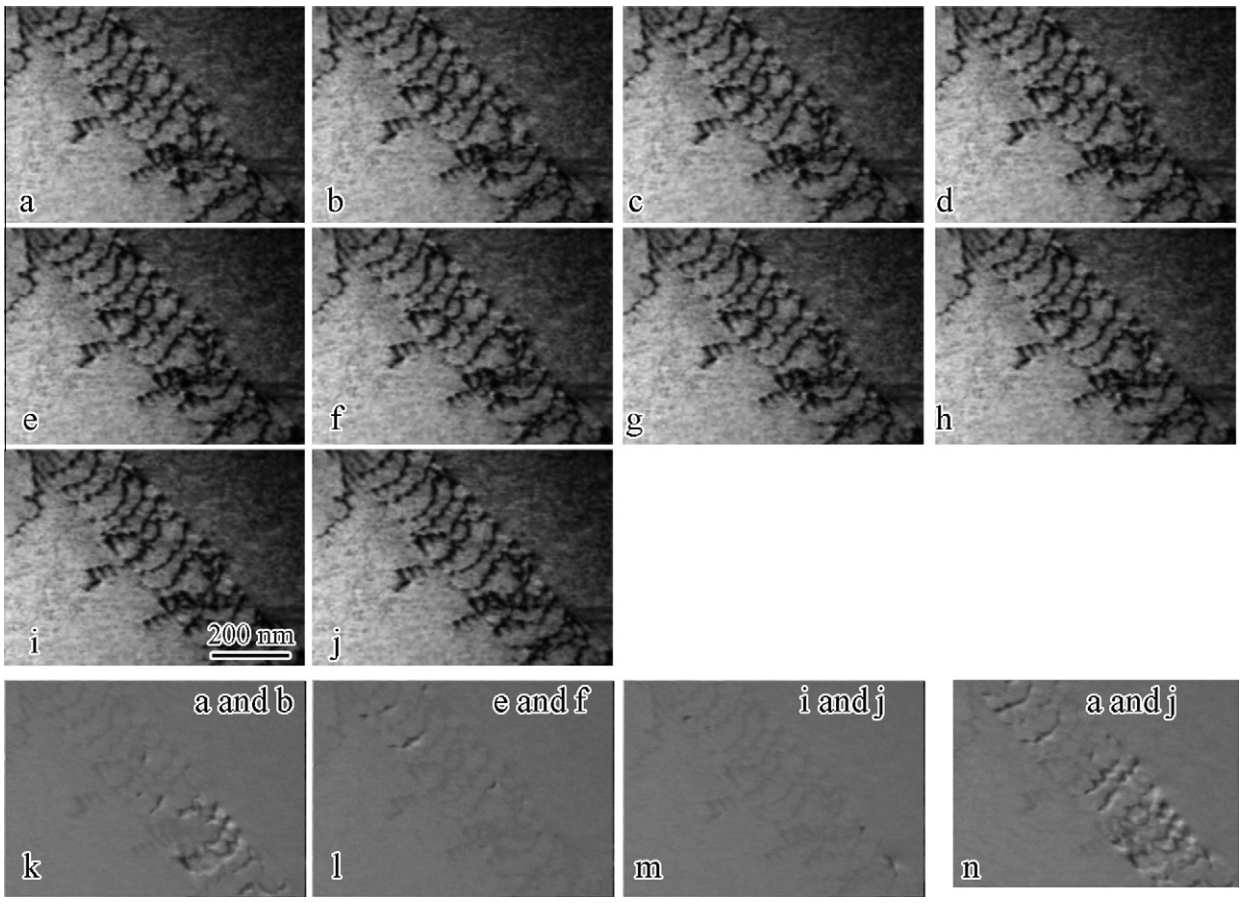

Fig. 5. Time-resolved series of images showing dislocation motion on the same slip band as in Fig. 1 after extensive dislocation motion. The time difference between each successive image was 10 s.

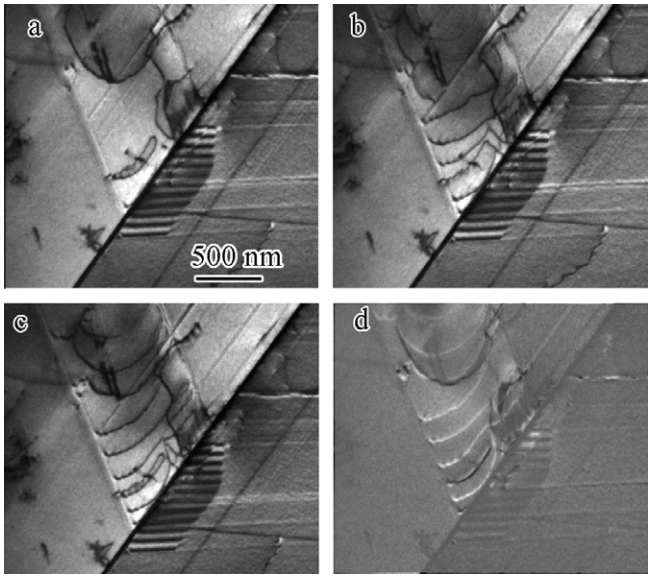

Fig. 6. Time-resolved series of images showing dislocation motion in unirradiated material. The time difference between each successive image was 5 s.

illustrate this difference a time-resolved series of images of dislocations approaching a grain boundary and forming a pile-up in the unirradiated and irradiated materials are compared in Fig. 7. From this comparison, it can be seen that in the unirradiated case the dislocation motion occurs over a shorter timeframe than in the irradiated case, and the dislocation images are smooth lines as opposed to the pinned and bowed segments that comprise the line dislocations in the irradiated case. With increasing dose the effect of the obstacle field increases and this changes the dislocation spacing in the pile-up and the distance the dislocations move in a given time. For example, for the dislocations indicated in the difference images the projected distance moved was 251 nm, 30 nm and 32 nm in 0.033 s, 0.866 s and 10.64 s, in the unirradiated, and irradiated to a dose of 5×10^{12} ions cm^{-2} and 5×10^{13} ions cm^{-2}, respectively. Of course, this result needs to be interpreted with the caveat that the loading is not necessarily the same for the two cases. However, these conclusions appear to hold for all conditions examined. From the images in Fig. 7, the nature of the interaction between the dislocations and grain boundary also appears to be influenced by the irradiation. In the unirradiated case, a conventional dislocation pile-up is observed forming at the grain boundary, whereas in the irradiated case the dislocations are more uniformly spaced as they approach the grain boundary and the rate of approach is slower requiring a higher shear stress to drive the dislocations to the grain boundary. A more detailed comparison and discussion of the interaction of dislocations with grain boundaries in unirradiated and irradiated materials will be presented elsewhere [26].

It was implied in the discussion of Figs. 2–4 that dislocation sources such as those in the vicinity of the crack tip and at grain boundaries were not impacted by the irradiation and continued to operate with minimal increases in applied load. Snapshots in time of the operation of a grain boundary source are shown in

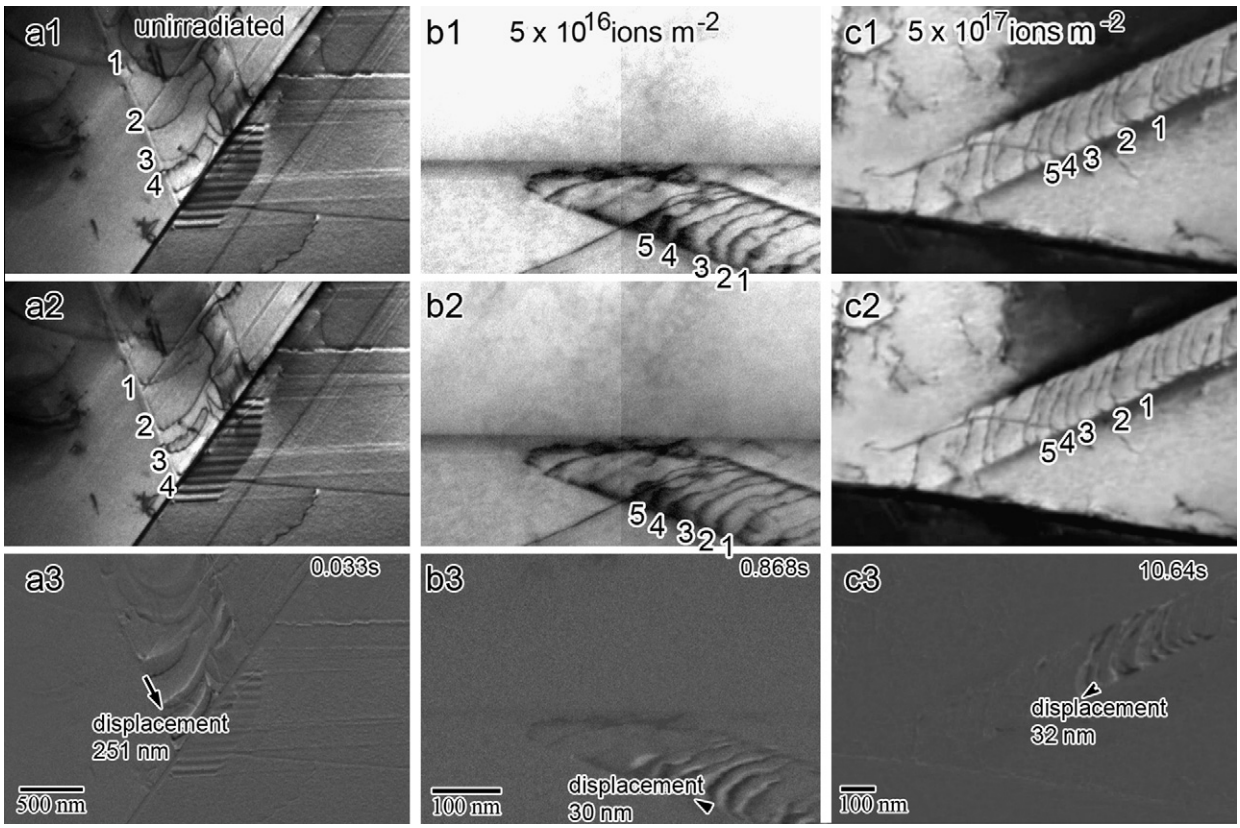

Fig. 7. Development of dislocation pile-ups at grain boundaries as a function of ion dose. (a) 0, (b) 5×10^{16} ions m^{-2}, and (c) 5×10^{17} ions m^{-2}.

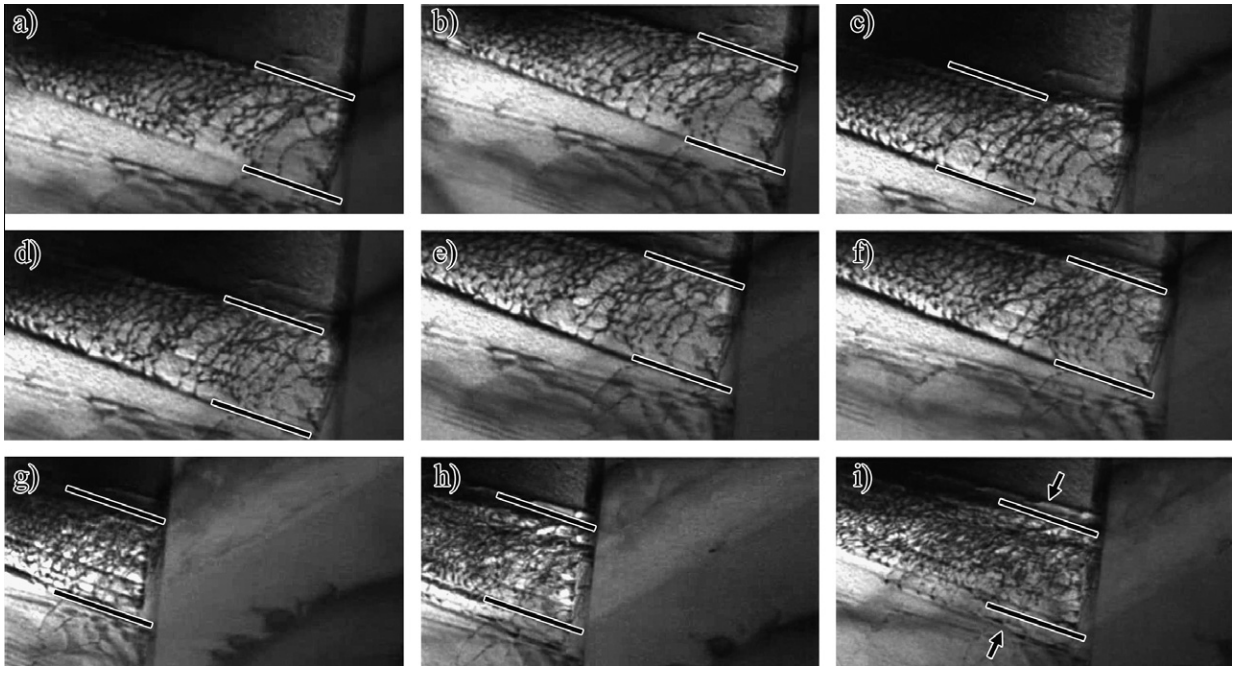

Fig. 8. Dislocation emission from a grain boundary source as a function of time following irradiation. Lines delineate the initial extremes of the slip planes emanating from the grain boundary.

Fig. 8. These images illustrate that the rate of emission of dislocations from the grain boundary as judged from the change in the dislocation structure near it, is very rapid and many dislocations are ejected. These dislocations do not propagate far from the source. Also, it appears that the width of the emission region from the grain boundary increases with source operation time. This can be seen by comparing the positions of the slip band intersections with the free surface. The lines superimposed on each image

indicate the intersections of the initial slip systems with the free surfaces. Clearly, there is an increase with increased straining such that the source can be viewed as occurring from within a volume element of the grain boundary with multiple emission points. The emission points need not and most likely do not operate continually as the magnitude of the back stress from the emitted dislocations may change with time and this might shut-down one emission point, at least temporarily, and activate another. This widening of the region of the grain boundary from which dislocations are emitted could have important consequences for determining the width of the defect-free channel.

4. Discussion

Central to the development of a model to account for the salient features of the changes observed in stress–strain curves as a function of irradiation dose is identification of the source of the dislocations responsible for the plastic response of the material. In this series of time-resolved experiments, it has been shown that:

- mobile dislocations are rendered immobile by the irradiation-produced defects;
- dislocation sources at grain boundaries and stress concentrators such as crack tips continue to pump dislocations into the lattice at a rate that appears unaffected by the irradiation-produced defects;
- dislocation mobility is hindered by the defects and the characteristics of motion are altered as the dislocations must percolate through the defect field, which results in the defects being reduced and eventually annihilated; and
- dislocation pile-ups at grain boundaries form at higher stresses in irradiated than in unirradiated metal.

The immobilization of the pre-existing glissile dislocations is shown to be a direct consequence of the irradiation defects increasing the shear stress needed to enable them to break away from the obstacle field. Here the dislocation interactions with individual defects were not resolved and therefore there was no measure of the breakaway strength. However, Robach et al. measured, from the curvature of the dislocation immediately prior to breakaway, the strength of the interaction of a dislocation with individual Frank loops in ion irradiated copper and found that the obstacle strength varied from 15 to 170 MPa with a mean of 40 MPa [11]. The variation in the barrier strength was related to the details of the interaction, namely, the dislocation type and the position at which the slip plane intersects the barrier. Such variability in the barrier strength would account for the discontinuous segmented dislocation motion that is observed in the images presented in Figs. 3–5.

The observation that the same dislocation source continues to produce dislocations on the same slip plane, Figs. 2 and 3, suggests that the local shear stress never attains the requisite value at the front of the dislocation array as the freshly generated dislocations never reach, and therefore do not influence, the leading dislocations. This result suggests that the rate-limiting step is not the nucleation of dislocations from sources such as grain boundaries but rather is the stress to propagate the dislocations through the field of obstacles. This conclusion has several important implications in regard to attributing the macroscopic stress–strain curves in terms of the behavior of dislocations.

Based on the observations presented herein, an understanding of the evolution of the dislocation structure within an individual grain emerges as shown in the series of schematics presented in the first column in Fig. 9. Here the continued operation of a grain boundary source is represented by a high density of dislocations accumulating at the source end of the grain, Fig. 9b. The difficulty of the dislocations, under the applied displacement, to propagate through the field of obstacles is represented by them moving partially through the grain, Fig. 9b. With continued loading the dislocations reach the boundary on the other side of the grain and a pile-up is formed, Fig. 9c. This pile-up is distinct from ones formed in unirradiated grains as the spacing is rather uniform as opposed to decreasing rapidly as the grain boundary is approached. With further increases in the load a more conventional pile-up will develop at the grain boundary

As the dislocations interact with and eventually annihilate the defects, the resistance to moving a dislocation along the slip plane attributable to the defects decreases with the passage of each dislocation. That is, the resistance is not a constant, but decreases as the strain increases. This decrease was apparent from the change in dislocation behavior represented in Figs. 3–5 in which the dislocation motion was seen to change with continued passage of dislocations. These concepts are illustrated schematically in the second column in Fig. 9, in which the dependence of the friction stress opposing dislocation motion as well as the defect density in a channel are shown as a function of distance between the source and barrier for three situations, irradiated but no slip, partial slip through the grain and complete slip through the grain. To test this concept and to explore the effect of having an increasing resistance to dislocation slip along a cleared channel, two-dimensional discrete dislocation dynamics simulations were used. For this preliminary simulation, the following assumptions were made: plane strain conditions hold, a constant macroscopic shear stress of 300 MPa was applied, dislocations were introduced until the back stress from the dislocation array halted operation, and the barrier was assumed to be insurmountable. The movement of individual dislocations was evaluated using the current velocity of dislocations, which was considered to be proportional to the Peach–Koehler force. The friction stress opposing dislocation motion along a slip plane in an unirradiated material was assumed to be constant and taken as $f^0_{unirr} = 10^{-3}\,G$ where $G = 76.9$ GPa is the shear modulus. For the irradiated material, the friction stress was assumed to increase linearly along the slip plane and, for this calculation, it is taken to increase linearly from $f^0_{irr} = f^0_{unirr} = 10^{-3}\,G$ near the source to $f^1_{irr} = 5 \times 10^{-3}\,G$ close to the barrier. Comparison of the dislocation pile-ups at steady state in the unirradiated and irradiated simulated materials is made in Fig. 10. Several differences are noted. Fewer dislocations were nucleated in the irradiated than in the unirradiated material, the form of the dislocation pile-ups were different, with a classical pile-up arrangement forming in the unirradiated but not the irradiated, and the dislocation spacing in the pile-up was greater in the irradiated than in the unirradiated material. These structures are consistent with the arrangements observed in the unirradiated and irradiated materials, see Fig. 7b and c. Increasing the magnitude of the barrier in the simulation of the irradiated material, results in the dislocations being halted before reaching the physical barrier. This result is consistent with the observation in Fig. 8 that the dislocations accumulate close to the source because of the magnitude of the barrier in the channel.

A consequence of having dislocation dynamics being controlled by the propagation stress rather than the nucleation stress is that in systems in which the obstacle density is high, a distinct yield point may appear even in FCC metals. It has been suggested that this simple explanation is incorrect as cleared channels have been observed in samples prior to the yield point drop being reached [24]. However, this observation simply reflects that the manifestation of a yield point drop in a macroscopic test requires a significant number of events to occur before it is reflected in such a test.

The observations reported in Fig. 2 suggest pre-existing dislocations, even if they were mobile prior to the irradiation are locked in position by the irradiation. By extension, it is suggested that any

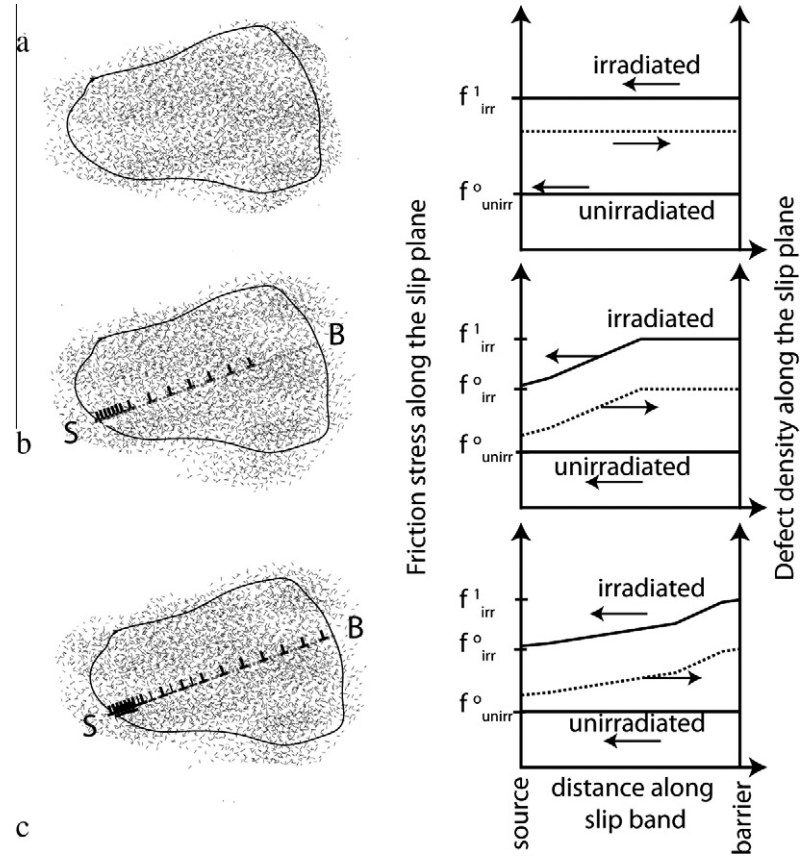

Fig. 9. Schematic illustration of the evolution of the dislocation structure within a channel and the corresponding change in the fraction stress with the channel as a function of strain.

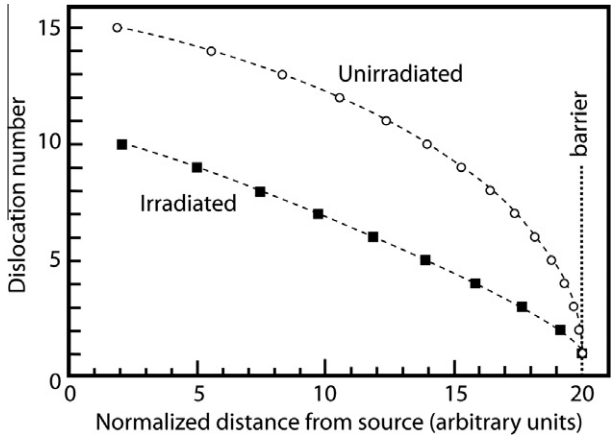

Fig. 10. Dislocation distribution against a barrier in a dislocation dynamics simulation of unirradiated and irradiated material. The friction stress opposing dislocation motion is constant in the unirradiated and increases linearly as the barrier is approached in the irradiated.

pre-irradiation Frank-Reed sources will be shut-down by the irradiation and new sources must be generated to create the defect-free channels. Further support for this shutting down of pre-existing sources comes from the nature of the dislocation motion through an obstacle field. Here it was demonstrated that dislocations move in a discontinuous manner and not as a unit as would be necessary for a source to operate. Of course, at sufficiently high levels of stress or at high strain rates such sources could be reactivated and they would then become competitive with the other sources.

Cleared channels in irradiated metals have a width in the range from 50 to 150 nm. Several dislocation processes have been proposed to explain how this channel width arises. For example, Diaz de la Rubia et al. used dislocation dynamics simulations to investigate the formation of defect-free channels [3]. From these simulations, it was suggested that the channel width was controlled by dislocations cross-slipping during the process of interacting with and annihilating the defects. Hiritani et al. suggested that in metals in which the primary defects were stacking-fault tetrahedra, the tetrahedra collapsed to Frank loops which caused interacting dislocations to double cross-slip [27]. Certainly, cross-slip processes have been observed when dislocations interact with an individual stacking-fault tetrahedron and this will cause a change in the position of the slip band within the channel [28]. Such processes will increase the field of obstacles with which the dislocations interact and would provide a mechanism for widening the channel. However, it is not obvious that cross-slip processes are sufficient to yield the wide channels that are observed experimentally. Finally, Ghoniem et al. proposed a different mechanism for widening the channel, namely, that the absorption of the vacancies from the stacking-fault tetrahedron by the dislocation caused the formation of jogs on it [14]. Here the distance between the source and the nearest grain boundary was important as this determined the number of possible interactions and the magnitude of the jog, which in turn sets the channel width. However, dislocations with such large jogs are not observed readily. Each of these models deals with the case in which the irradiation-produced defects are stacking-fault tetrahedra, but defect-free channels are formed independent of the nature of the defects and a more general explanation may be needed.

The current observations offer an alternate explanation that is independent of the material and the nature of the defects. From the images in Fig. 8, it is suggested that the dislocation source in the grain boundary is not a line but a volume element and it is not static in the sense that emission from one region can be shut-down temporarily and a new nearby source activated. This mechanism provides generation of dislocations of the same type on parallel slip planes and a natural explanation for the variable width of the channel. Similarly, dislocation sources at a crack tip can generate many dislocations on multiple parallel slip planes as seen, for example, in the work of Robach et al. [11]. It remains to be verified that the dislocation source width is sufficient to account for the channel width or if supplementary processes such as cross-slip or jog formation are required too.

The interaction of dislocations in the channel have important consequences for generating conditions for activating grain boundary sources and, as suggested by Was and Busby, of generating conditions that may be favorable for nucleating a grain boundary crack, which has important implications for the sensitivity of steels to stress corrosion cracking [15]. The work reported herein did not emphasize this component of the interaction but differences in response of grain boundaries in unirradiated and irradiated metals were observed. First, the development of dislocation pile-ups at a grain boundary occurred at higher applied loads in irradiated than in unirradiated metals, which simply reflects the difficulty of continuing to percolate those first dislocations through the obstacle field towards the grain boundary. The continued uninterrupted operation of the dislocation source and the difficulty of propagating these dislocations through the obstacle field generate a situation in which the dislocation density close to the source is high, Fig. 8. This is the reverse of the normal dislocation distribution against a barrier. The back stress from these dislocations can cause the source to cease operation and for a new source to be generated at another location along the grain boundary. Alternatively, it is feasible that this could cause the boundary to adopt another relief mechanism, namely, the generation of a grain boundary crack or establish the necessary stress conditions to rupture the oxide at this location. This concept is the subject of further investigation.

5. Conclusions

By conducting ion irradiation as well as straining experiments *in situ* in the transmission electron microscope it has been demonstrated that dislocations mobile prior to the irradiation are effectively locked in position by the irradiation-produced defects. This result has implications for the models developed to explain the degradation in the mechanical properties of irradiated metals and suggests that the physical basis of these models may need to be revisited as the dislocations responsible for generating the defect-free channels must be newly generated and cannot be sources constructed from motion and interaction of pre-existing dislocations.

In contrast, dislocation sources associated with grain boundaries or stress concentrators such as a crack tip appear to be unaffected by the presence of the defects and continue to nucleate and release dislocations. This implies the rate-limiting step is the dislocation propagation not the nucleation stress. The mobility of these dislocations is altered by the presence of the defects to such an extent that the motion is slow and jerky as the dislocations have to percolate through the obstacle field. The increase in applied stress is now most likely associated with the need for a higher shear stress to push the dislocations through the obstacle field. With continued passage of dislocations, the velocity increases as the defects are either annihilated or fragmented by the passage of successive dislocations. This observation suggests that the stress to move dislocations through the obstacle field will decrease with time, which initially could give rise to the presence of an apparent yield point drop.

Acknowledgements

This work was supported by the US Department of Energy, Office of Basic Energy Sciences under Contract No. DE-FG02-08ER46525. The authors thank Grace Liu and Josh Kacher for the images presented in Fig. 1 and Dr. M.A. Kirk for his assistance, support and for many fruitful discussions. The authors would like to acknowledge the use of the IVEM-accelerator facility at Argonne National Laboratory. This document was prepared by the University of Illinois at Urbana-Champaign as a result of the use of facilities of the US Department of Energy (DOE), which are managed by UChicago Argonne, LLC, acting under Contract No. DE-AC02-06CH11357. Neither UChicago Argonne, DOE, the US Government, nor any person acting on their behalf: (a) make any warranty or representation, express or implied, with respect to the information contained in this document; or (b) assume any liabilities with respect to the use of, or damages resulting from the use of any information contained in the document.

References

[1] A. Almazouzi, T. Diaz de la rubia, B.N. Singh, M. Victoria, J. Nucl. Mater. 276 (2000) 295–296.
[2] C. Bailat, F. Groschel, M. Victoria, J. Nucl. Mater. 276 (2000) 283.
[3] T. Diaz de la Rubia, H.M. Zbib, T.A. Khraishi, B.D. Wirth, M. Victoria, M.J. Caturla, Nature 406 (2000) 871–874.
[4] T.A. Khraishi, H.M. Zbib, T. Diaz de la Rubia, M. Victoria, Metall. Mater. Trans. B Process Metall. Mater. Process. Sci. 33B (2002) 285–296.
[5] G.E. Lucas, Irradiation-induced changes in the mechanical properties and microstructures of solution annealed austenitic stainless steel at low to intermediate temperatures, in: I.M. Robertson, G.S. Was, L.W. Hobbs, T. Diaz de la Rubia (Eds.), Microstructure Evolution During Irradiation, 1997, pp. 425–436.
[6] B.N. Singh, D.J. Edwards, P. Toft, J. Nucl. Mater. 299 (2001) 205–218.
[7] B.N. Singh, N.M. Ghoniem, H. Trinkaus, J. Nucl. Mater. 307–311 (2002) 159–170.
[8] B.D. Wirth, M.J. Caturia, T. Diaz de la Rubia, T. Khraishi, H. Zbib, Nucl. Instrum. Methods Phys. Res. Sect. B-Beam Interact. Mater. At. 180 (2001) 23–31.
[9] H.M. Zbib, T. Diaz de la Rubia, M. Rhee, J.P. Hirth, J. Nucl. Mater. 276 (2000) 154–165.
[10] M. Victoria, N. Baluc, C. Bailat, Y. Dai, M.I. Luppo, R. Schaublin, B.N. Singh, J. Nucl. Mater. 276 (2000) 114–122.
[11] J.S. Robach, I.M. Robertson, B.D. Wirth, A. Arsenlis, Philos. Mag. A 83 (2003) 955–967.
[12] I.M. Robertson, J.S. Robach, H.J. Lee, B.D. Wirth, Acta Mater. 54 (2006) 1679–1690.
[13] A. Arsenlis, B.D. Wirth, M. Rhee, Philos. Mag. 84 (2004) 3617.
[14] N.M. Ghoniem, S.H. Tong, B.N. Singh, L.Z. Sun, Philos. Mag. A 81 (2001) 2743–2764.
[15] G.S. Was, J.T. Busby, Philos. Mag. 85 (2005) 443–465.
[16] Y. Matsukawa, Y.N. Osetsky, R.E. Stoller, S.J. Zinkle, Mater. Sci. Eng. A (Struct. Mater.: Prop., Microstruct. Process.) 400–401 (2005) 366–369.
[17] Y. Matsukawa, Y.N. Osetsky, R.E. Stoller, S.J. Zinkle, J. Nucl. Mater. 351 (2006) 285–294.
[18] Y.N. Osetsky, D. Rodney, D.J. Bacon, Philos. Mag. 86 (2006) 2295–2313.
[19] Y.N. Osetsky, R.E. Stoller, Y. Matsukawa, Dislocation-stacking fault tetrahedron interaction: What can we learn from atomic-scale modelling, in: Proceedings of the 11th Conference on Fusion Research, Elsevier, Amsterdam, Netherlands, Kyoto, Japan, December 7-12-2003, 2004, pp. 1228–1232.
[20] D. Rodney, Nucl. Instrum. Methods Phys. Res. Sect. B-Beam Interact. Mater. At. 228 (2005) 100.
[21] L.Z. Sun, N.M. Ghoniem, S.H. Tong, B.N. Singh, J. Nucl. Mater. 283–287 (Part B) (2000) 741–745.
[22] B.D. Wirth, V.V. Bulatov, T. De La Diaz Rubia, J. Eng. Mater. Technol., Trans. ASME 124 (2002) 329.
[23] B.D. Wirth, V.V. Bulatov, T. Diaz de la Rubia, Atomistic simulation of dislocation-defect interactions in Cu, in: Microstructural Processes in Irradiated Materials, 2000, R.3.27.21-26.
[24] D.J. Edwards, B.N. Singh, J.B. Bilde-Sorensen, J. Nucl. Mater. 342 (2005) 164–178.
[25] J.I. Cole, S.M. Bruemmer, J. Nucl. Mater. 225 (1995) 53–58.
[26] M. Bricena, J. Fenske, I.M. Robertson, 2010, unpublished data..
[27] M. Hiratani, H.M. Zbib, B.D. Wirth, Philos. Mag. 82 (2002) 2709–2735.
[28] M. Briceno, I.M. Robertson, Unpublished work, 2010.